UNIABUJA Journal of Engineering and Technology
https://ujet.uniabuja.edu.ng/
ISSN: 2714-3236 (Online); 2714-3228 (Print)
Volume 3, Issue 1, 2026; 198-211

Deployment of Unified Power Quality Conditioner in a 33 kV Distribution Network Using MFO-ANFIS

Chioma M. OGBOKE[1*], Muhammad UTHMAN[2], Abdullahi S.B. MOHAMMED[3], Prince C. UDEH[4]

[1*,2,3]*Department of Electrical/Electronic Engineering, University of Abuja, Abuja, Nigeria*
[4]*Department of Electrical/Electronic Engineering, Veritas University Abuja, Abuja, Nigeria*

[1*]*chiomaene2013@gmail.com*, [2]*m.uthman@yahoo.com*, [3]*abdullahi.mohammed@uniabuja.edu.ng*, [4]*udeh.p@veritas.edu.ng*

Abstract
Power quality issues are often experienced along distribution lines. These challenges are in the form of voltage sag and swells, excessive power losses, and harmonic distortions at common points. Faults and non-linear loads are mostly responsible for introducing these power qualities which can be experienced as harmonics. Harmonics affect the quality of power on the affected lines or other parallel loads. The Unified Power Quality Conditioner (UPQC) has emerged as a promising solution to these power quality issues. The UPQC comprises of the Dynamic Voltage Restorer (DVR) for voltage related issues, and the Distribution Static Compensators (DSTATCOM) for current related issues. In this paper, the UPQC and a 33kV three-phase four wire distribution line of system are designed using MATLAB/Simulink. Simulink as a three-phase four-wire system. The DVR and DSTATCOM are designed using a 3-phase universal gate in IGBT mode as series and shunt filter respectively. The former compensates foe voltage sag or swell while the latter, compensates the current levels. One crucial component is a controller for the UPQC and this is done using a Moth-Flame Optimized Adaptive Neuro-fuzzy Inference System (MFO-ANFIS). The study compared the total harmonic distortion (THD) at the Point of common coupling (Pcc) in the current for two scenarios – without UPQC, and with MFO-ANFIS-controlled UPQC. The MFO-ANFIS performed very well with THD of 7.02% which is within the acceptable standards of IEEE-519.

Keywords: *Initial ANFIS, Distribution lines, MFO, Power Quality, UPQC.*

1.0 Introduction

While power systems are designed to be reliable and safe, a number of unpredictable factors could easily cause power quality issues. Power quality (PQ) could be defined as any power related issues resulting in abnormal behavior of equipment, impeding power quality. It could be in the form of voltage sag and swell, harmonics, excessive power losses. The quality of the electric power supply has been significantly impacted by the development of power electronic-based devices which, when functional produce harmonics, creating power issues. Unified power quality conditioner (UPQC) which incorporate active power filters (APFs) has emerged as a solution to enhancing power quality. In this study, unified power quality conditioner (UPQC) was deployed using moth flame optimization algorithm and ANFIS (MFO-ANFIS) to mitigate power quality problems in a 33kV distribution feeder. The diagrammatic representation of UPQC is shown in figure 1.

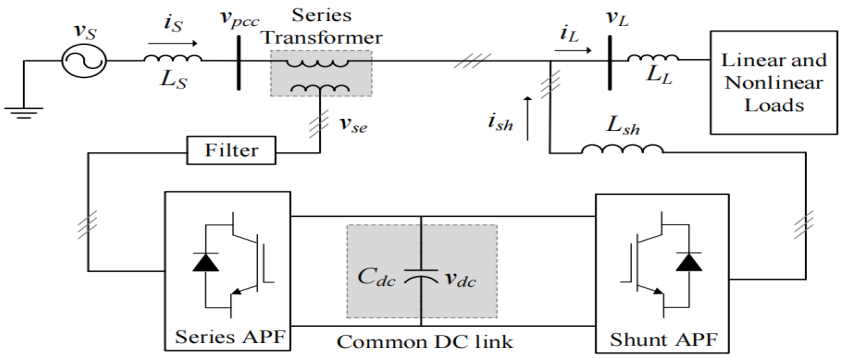

Figure 1. Basic Representation of UPQC (Chaiyaphun et al., 2024).

According to their system configuration, active power filters can be divided into two categories: series and shunt. Shunt APFs reduce current-based distortions, while series APFs deal with voltage-based distortions. The UPQC is a series and shunt active power filter combination: voltage and current-based

Received: 20-10-2025 / Accepted: 13-10-2025 / Published: 13-02-2026

https://doi.org/10.70118/ujet.2026.0301.19

waveform distortion are both reduced simultaneously. The shunt APF represents a Distribution Static Compensator (DSTATCOM) while the series APF is the Dynamic Voltage Restorer (DVR). The purpose of the DSTATCOM coupled parallel to the network and load in a three-phase network, is to cancel load harmonics fed to the supply. It works as a current source, generating the harmonic currents the load requires to balance them in addition to providing reactive power. In order to compensate for undesirable components of the load current the DSTATCOM injects currents into the point of common coupling (PCC). Its benefit is that it simply entails compensation - current plus a small amount of active fundamental current supplied to compensate for system losses as shown in figure 2.

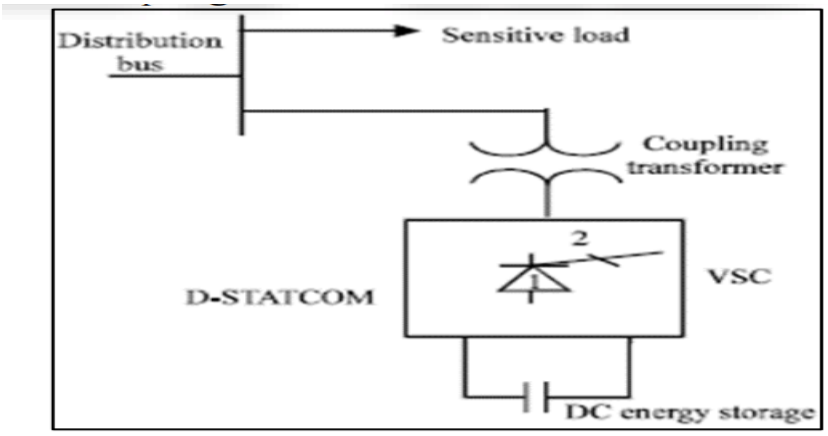

Figure 2. Distribution Static Compensator (DSTATCOM) (Mishra and Kumar, 2017).

DVRs inject a voltage component in series with the supply voltage to account for voltage sags and swells on the load side. The ability to inject voltage into any phase with respect to the load current implies active power transfer capabilities. This active power that is transmitted via the dc connection can be produced by a diode bridge connected to the ac network, a PWM converter connected to a shunt, or an energy storage device. In addition to balancing the voltages and providing voltage, it serves as a harmonic isolator to prevent harmonics from entering the source voltage and reaching the load. Figure 3 shows the DVR.

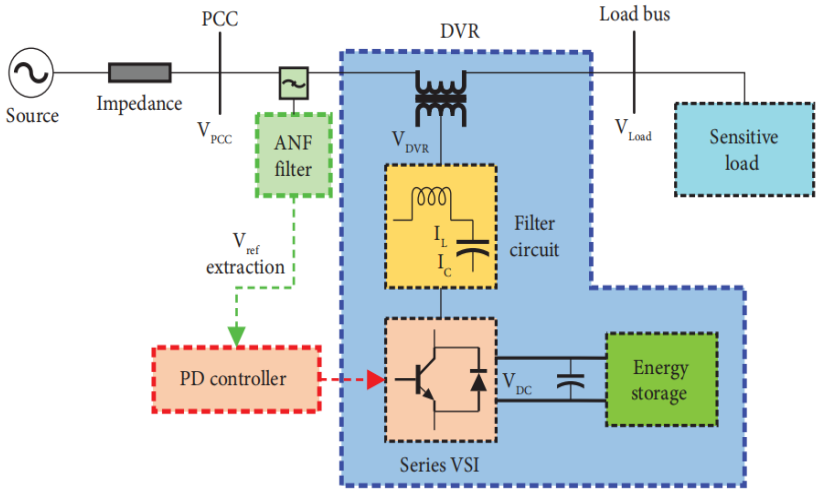

Figure 3. Dynamic Voltage Restorer (DVR) (Alrashad et al., 2024).

Harmonics, reactive power, negative-sequence current, supply voltage flicker, and imbalance are accounted for primarily by UPQCs. So, at the point of installation on power distribution or industrial power systems, the UPQC can improve power quality. The UPQC is therefore expected to provide solutions for delicate large capacity loads. The UPQC is projected to be one of the most effective modern power devices to provide solutions to large capacity loads sensitive to supply voltage and load current disturbances/imbalance. It can concurrently correct for unbalance and distortion in both the source voltage and the load current (Srimatha et al., 2023), unlike the other devices, DSTATCOM and DVR which can only correct either current or voltage distortion respectively.

Some body of literature exist for works done with UPQC. Chaiyaphun et al. (2024) proposed a modified harmonic identification of the UPQC in a bid to mitigate the challenges posed by the distorted supply voltage

Received: 20-10-2025 / Accepted: 13-10-2025 / Published: 13-02-2026

https://doi.org/10.70118/ujet.2026.0301.19

which affect the control performance of a UPQC. Here, the reference compensating current calculation for the shunt active power filter (shunt APF) is developed using the sliding window with the Fourier analysis (SWFA) method.

Sundarabalan et al. (2019) proposed an ANFIS controller to enhance the power quality of a fuel cell integrated unified power quality conditioner (FCI-UPQC). Results from the study suggest that the proposed FCI-UPQC compensated power quality problems such as voltage sag, swell, harmonics, neutral current, source current imbalance in a three-phase four-wire distribution grid. Srimatha et al. (2023) also proposed an ANFIS-based system, intelligent ANFIS-based DC voltage controller for customized UPQC devices with the aim of mitigating the existing power quality challenges by reducing the issues in classical controllers and incorporating intelligence knowledge with subjective decisions. The study and simulations were implemented in MATLAB.

Afonso et al. (2021) presented an extensive review on power electronics technologies applied to power quality improvement. The review highlighted the main phenomena associated with the occurrence of power quality problems in smart grids, their cause and effects for different activity sectors, and the main power electronics topologies for each technological solution.

Kenjrawy et al. (2022) proposed a new modulation technique for a nine-level structure for a standardized power quality conditioner. The conditioner is connected between a photovoltaic system (UPQC-PV) and a smart grid. The study was implemented in MATLAB/Simulink for different disturbance scenarios. Nicola et al. (2023) proposed a method of improving the performance of UPQC by comparatively analyzing the performance when using a Proportional Integrator (PI)-type controllers optimized by a Grey Wolf Optimization (GWO) computational intelligence method, fractional order (FO)-type controllers based on differential and integral fractional calculus, and a PI-type controller in tandem with a Reinforcement Learning—Twin-Delayed Deep Deterministic Policy Gradient (RL-TD3) agent. Huang et al. (2022) discussed the restructuring of the distribution networks optimally for UPQC. The study also determines the most appropriate branch where the UPQC must be located and the most appropriate reactive power size with which the series and shunt filters must be injected into the grid. The simulations were applied to 69- and 84-standard-bus networks. Mohamed et al. (2018) presented a paper on how to operate a unified power quality conditioner at its best steady state for reducing power losses and enhancing voltage profiles. To determine the appropriate position and size of UPQC while keeping network restrictions, the goal is to decrease power losses and enhance voltage profile. Both active power and reactive power may be used to compensate for voltage. Amini and Alireza (2020) proved the effectiveness of the unified power quality conditioner in reducing power quality issues over other FACTS devices. Bharathi et al. (2017) examined how the UPQC could be optimally placed. A multi-objective stochastic planning is demonstrated for adjusting reactive power in radial distribution networks with wind generation using a unified power quality conditioner (UPQC). Biricik (2018) established that the greater use of delicate devices has an impact on the quality of the power transmitted. The study demonstrated a controller that employs UPQC to correct for voltage sag. Cek (2018) demonstrated how UPQC's performance may be improved by using a Self-Tuning Filter (STF) on the controller component in conditions of low grid voltage as well as current imbalance and distortion.

Xia et al. (2013) presented a low carbon, high efficiency and high quality power supply scheme for Distributed Generation (DG) in a micro-grid. A three-phase, four-leg DG grid-interfacing converter based on the improved structure of a Unified Power Quality Conditioner (UPQC, including a series converter and a parallel converter) was adopted.

Mirjalili (2015) investigated the moth flame optimization (MFO) algorithm's benefits and drawbacks were investigated. The study did however show that the MFO algorithm had issues such uneven exploration and exploitation, little population diversity, early convergence, and local optima trapping. The research recommended utilizing the improved moth-flame optimization (I-MFO) algorithm, which locates trapped moths in local optimums by specifying memory for each moth, to overcome the issues with canonical MFO. Banachaiba et al. (2014) used moth flame optimization algorithm to determine the optimal allocation of unified quality conditioner (UPQC) in the distribution system.

Dash and Pravat (2021) assessed the primary power quality issues and, the remedial steps that could be implemented. This paper explored the techniques for resolving supply voltage sag, swell, and interruption in a distributed system. Dharmalingam et al. (2014) showed that voltage instability is the main cause of the poor power quality in electric power systems. The enormous losses incurred at the distribution level of these systems, where 10–13% of the total generation is lost as heat, cause great worry among power system operators.

Hosseini and Meidi (2018) suggested the use of a Bacterial Foraging Algorithm (BFA) based method for optimal placement of UPQC. The investigation showed the effectiveness and viability of the strategy for integrating UPQC into real-world power distribution networks resulting in a 20.045% reduction in power quality issues.

Received: 20-10-2025 / Accepted: 13-10-2025 / Published: 13-02-2026

https://doi.org/10.70118/ujet.2026.0301.19

Tarani et al. (2018) investigated the placement, integration, capacity enhancement and real time control of the UPQC to improve the power quality (PQ) of a distributed generation network connected to the micro-grid. The study was implemented in MATLAB for a three phase four wire system.

Mahdi and Gorel (2022) used a UPQC with a sensitive load on the grid system to analyze the THD attenuation under different disturbances, using pulse-width modulation and hysteresis as switching techniques. Study was implemented in MATLAB/Simulink results show that electrical power is continuously fed to the load in all disturbances with total harmonic distortion (THD) less than 5% for voltage and 4.5% for current.

1.1 Load Flow Studies

For load flow studies the single diagram of the UPQC as shown in figure 4 is studied.

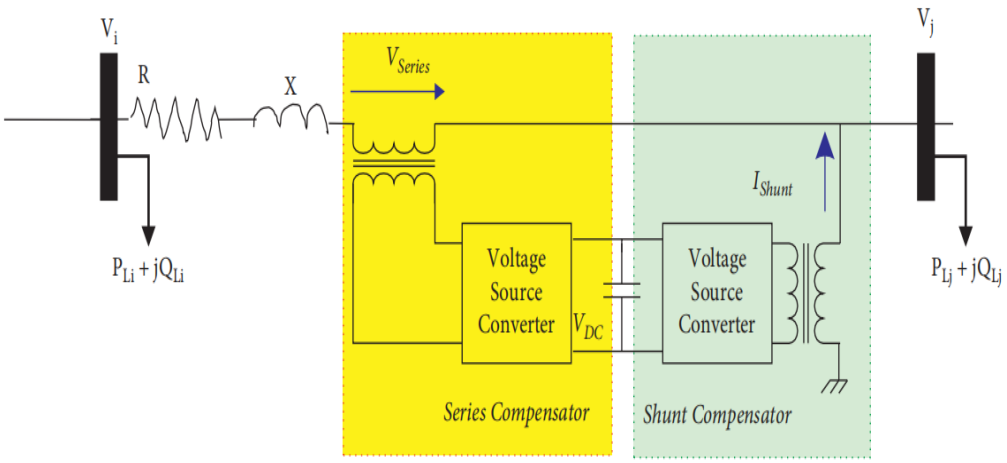

Figure 4. Single line diagram of the UPQC (Huang et al., 2022).

Figure 4 is transformed to its Thevenin equivalent as seen in figure 5.

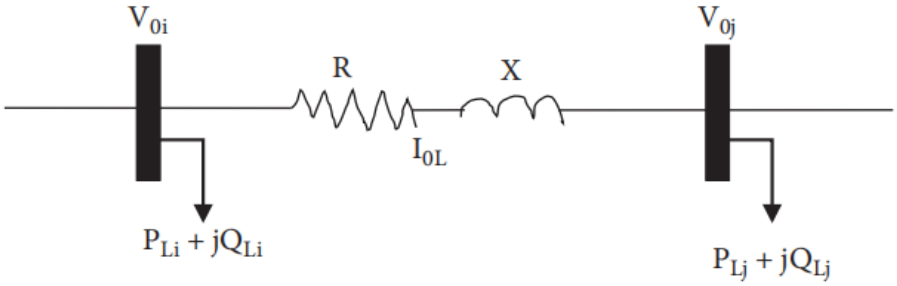

Fig. 5. Thevenin's equivalent circuit for UPQC (Huang et al., 2022).

If the network's Norton equivalent circuit is achieved from the points of *i* and *j*, the Thevenin's circuit becomes the Norton circuit as in figure 6.

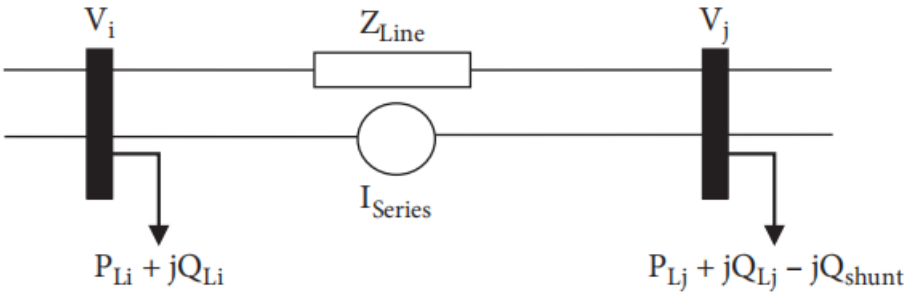

Figure 6. Norton's equivalent circuit for the series part of UPQC (Huang et al., 2022).

The injected series power can then be modeled as loads of *i* and *j* buses:

Received: 20-10-2025 / Accepted: 13-10-2025 / Published: 13-02-2026
https://doi.org/10.70118/ujet.2026.0301.19

$$I_s = \frac{V_s}{Z_s} \quad (1)$$

where *V*s, *I*s, and *Z*s are voltage, current, and impedance for buses, and these parameters are obtained as follows:

$$V_s = V_{sm} < \delta_{V_s} \quad (2)$$

$$I_s = I_{sm} < \delta_{I_s} \quad (3)$$

where δ_{V_s} and δ_{I_s} are the angle of voltage and current, respectively. V_{sm} and I_{sm} are the maximum values of voltage and current, respectively. Balanced power is required in the load flow, therefore the current source was replaced by equivalent power equations, and figure 6 becomes the load model in figure 7.

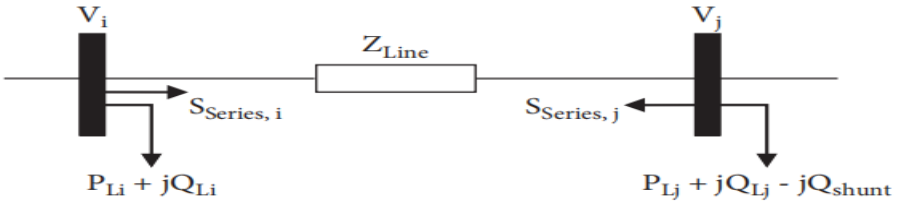

Figure 7. Load model for the series part of the UPQC (Huang et al., 2022).

The active power can now be obtained using:

$$S_{series,i} = V_i \times (-I_s^*) \quad (4)$$

$$P_{series,i} = real\{S_{series,i}\} \quad (5)$$

$$Q_{series,i} = Im\{S_{series,i}\} \quad (6)$$

where $S_{series,i}$ (VA), $P_{series,i}$ (W), and $Q_{series,i}$ (Var) are complex, active, and reactive power in the series lines, respectively. These operations were performed in each of the load flow iterations. The source current *Is* was calculated in each iteration is using:

$$I_s = \frac{V_{sm}}{|Z_m|} < \frac{V_i + \pi}{2} \quad (7)$$

After completing the load flow iterations, the injected series voltage angle was calculated using:

$$\delta_{V_s} = \left(\frac{I_s}{Zs}\right) \quad (8)$$

2.0 Materials and Method

MATLAB/SIMULINK is used to train the MFO-ANFIS model. The model consists of a 3-phase 4-wire (3PFW) 33kV distribution line built using three-phase sources and distributed parameter blocks. Voltage and current measuremet sensors were implemented using three-phase V-I measurement blocks, while the shunt and series active filters were designed using IGBTs. Control of the filters were done using an ANFIS subsystem for gate pulse generation. The block diagram for the model is in figure 8.

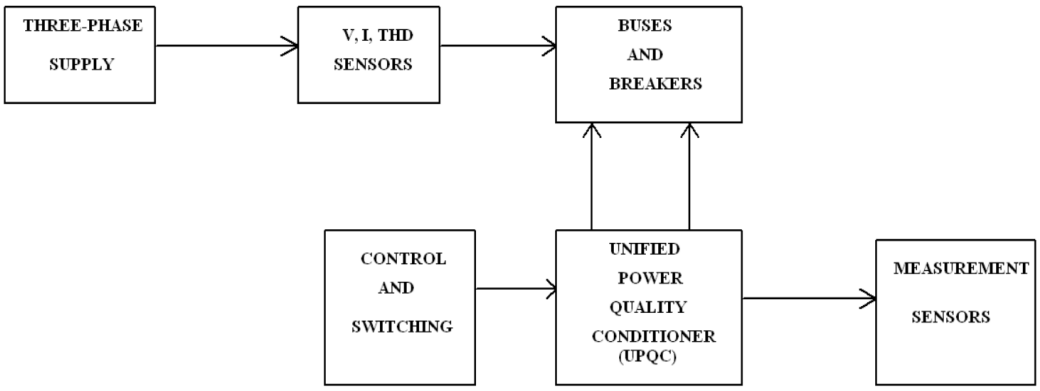

Figure 8. Block diagram of model.

Figure 9 shows the distribution line system as it was designed in SIMULINK. The source is the leftmost block while the UPQC system is at the bottom as shown by the inset description. The three-phase source, fault section, and load point are also shown.

Received: 20-10-2025 / Accepted: 13-10-2025 / Published: 13-02-2026

https://doi.org/10.70118/ujet.2026.0301.19

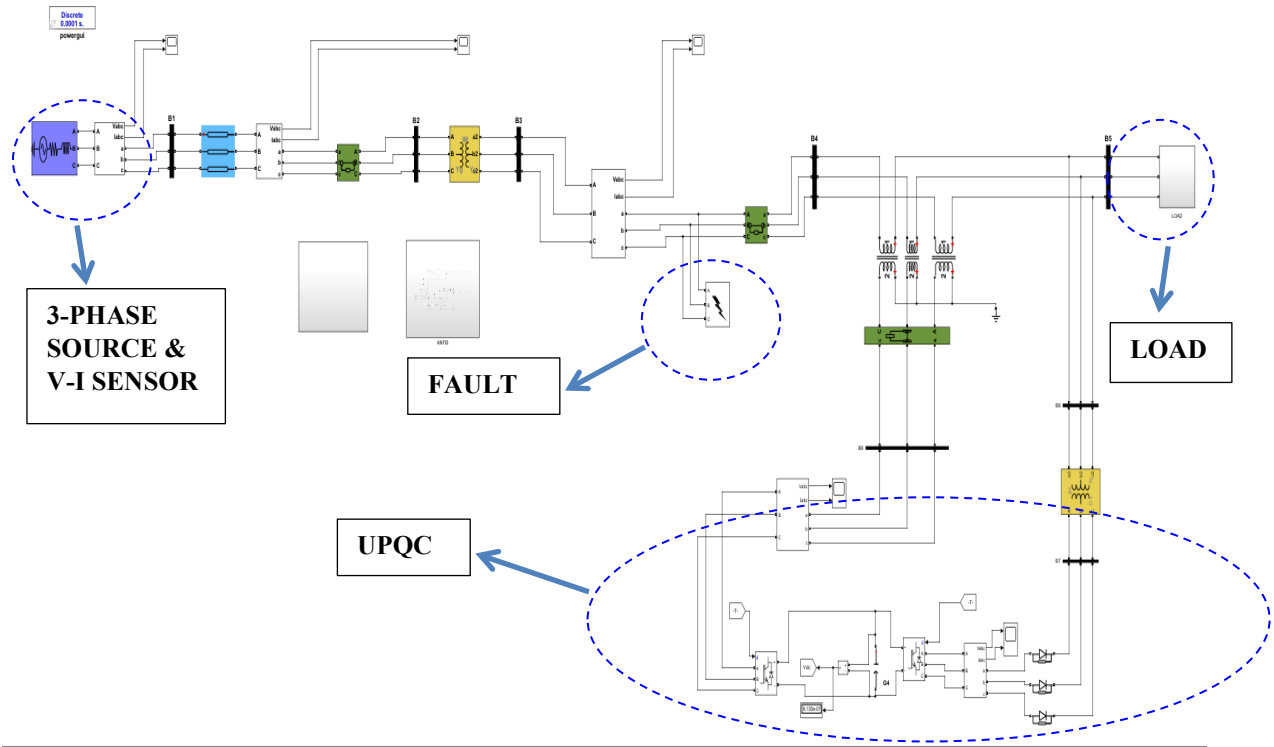

Figure 9. Distribution line with UPQC in SIMULINK

Figure 10 is the ANFIS subsystem in the model. The model was simulated for 0.5s with a L-G (single line-to-ground) fault. The fault was included to observe the impact of the UPQC in handling severe system disturbances.

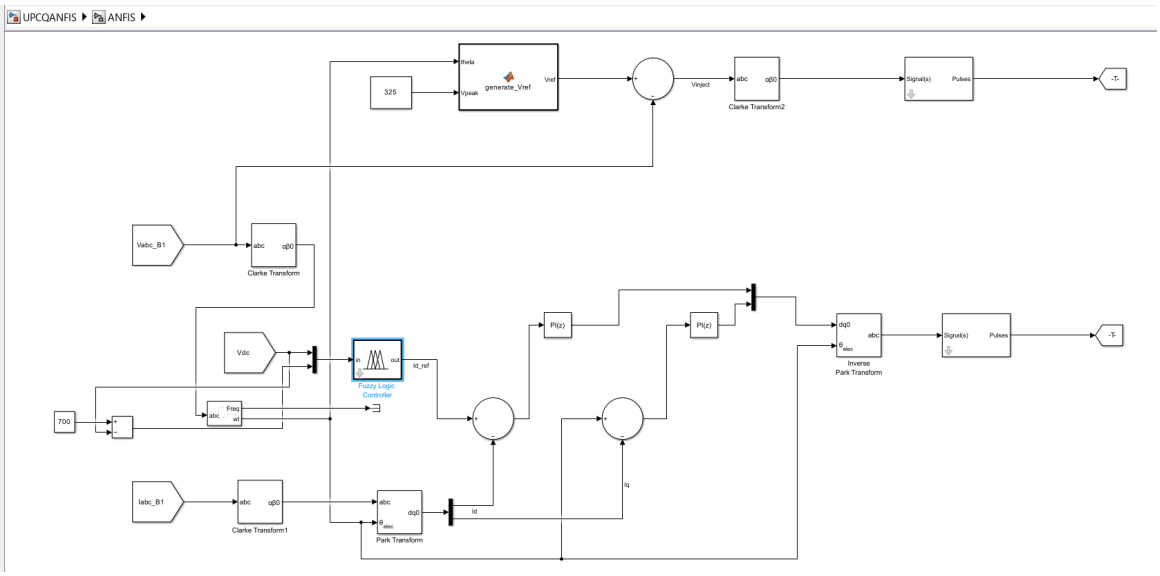

Figure 10. ANFIS Controller sub-system

A control scheme was required to fire the gate pulses for the shunt and series VSCs in the UPQC. The control scheme adopted here makes use of the synchronous reference frame and phase-locked loop to control the converters. The control process is presented next.

2.1 UPQC Control Scheme

2.1.1 Clarke transform (abc → $\alpha\beta$)

This was used to convert the three-phase signals (voltage or current) into 2-axis orthogonal signals, giving a 2D rotating vector in the stationary frame.

Received: 20-10-2025 / Accepted: 13-10-2025 / Published: 13-02-2026
https://doi.org/10.70118/ujet.2026.0301.19

$$\begin{bmatrix} V_\alpha \\ V_\beta \end{bmatrix} = \frac{2}{3}\begin{bmatrix} 1 & -\frac{1}{2} & -\frac{1}{2} \\ 0 & \frac{\sqrt{3}}{2} & -\frac{\sqrt{3}}{2} \end{bmatrix}\begin{bmatrix} V_a \\ V_b \\ V_c \end{bmatrix} \quad (9)$$

The injected voltage is obtained from the formula:

$$V_{injected} = V_{ref} - V_{abc} \quad (10)$$

where $V_{injected}$ is the voltage to be injected into the grid; V_{ref} is the reference voltage obtained from the desired nominal voltage value and obtained as in equation 11; V_{abc} is the source voltage.

$$V_{ref} = V_{peak}\left[sin\theta;\ \sin(\theta - \left(2 \times \frac{pi}{3}\right);\ \sin(\theta + \left(2 \times \frac{pi}{3}\right)\right] \quad (11)$$

The injected voltage undergoes a clarke transformation, and the extracted alpha and beta components were used to fire series pulses.

2.1.2 Park transform ($\alpha\beta \rightarrow dq0$ *or* $abc \rightarrow dq0$)

This rotates the αβ (or abc) components into a synchronous rotating frame, locking with the fundamental frequency. This made the fundamental component DC while the harmonics appear as AC ripple.

$$\begin{bmatrix} d \\ q \end{bmatrix} = \begin{bmatrix} cos\theta & sin\theta \\ -sin\theta & cos\theta \end{bmatrix}\begin{bmatrix} \alpha \\ \beta \end{bmatrix} \quad (12)$$

where theta θ is the angle of the rotating frame, obtained using a phase-locked loop tracking the supply voltage; d aligns with the active power and q aligns with the reactive power. The axis of d and q are orthogonal.

2.1.3 SRF control

SRF here stands for Synchronous reference frame which is a rotating coordinate system that rotates at the same frequency as the fundamental component (50Hz). The control strategy based on SRF for the Shunt APF and Series APF is presented here.

For shunt APF that is current compensation, the following procedure was followed:

1. Input: Load current which is three phase
2. Transform to Clarke and then Park to obtain i_d and i_q.
3. Set references

$$i_d^{ref} = I_{load\_d} \quad (13)$$

$$i_q^{ref} = 0 \text{ (reactive current reference is zero)} \quad (14)$$

$$e_d = i_d^{ref} - i_d \quad (15)$$

$$e_q = \ i_q^{ref} - i_q \quad (16)$$

where e_d and e_q are error components in the d-axis and q-axis respectively.

For series APF that is voltage compensation, the following procedure was followed:

1. Input: Voltage at point of common coupling (Pcc)
2. Transform to Clarke and then Park to obtain v_d and v_q.
3. Reference voltage v_d^{ref}

$$v_d^{ref} = V_{rated} \quad (17)$$

$$v_q^{ref} = 0 \text{ (reactive current reference is zero)} \quad (18)$$

$$e_{vd} = v_d^{ref} - v_d \quad (19)$$

$$e_{vq} = \ v_q^{ref} - v_q \quad (20)$$

where e_{vd} and e_{vq} are error voltage components in the d-axis and q-axis respectively. V_{rated} should be higher than the nominal voltage.

2.2 Network Architecture

The hybrid network architecture is described in table 1. The model consists of six layers as shown. Two control inputs (error value and its integral), 3 membership functions (MF), 9 firing rules which result in 9 outputs, and the output is a weighted sum.

Table 1. MFO-ANFIS Architecture

Layer	Name	Function	Optimized Parameter
1	Input layer	Receives 2 control input	---
2	Fuzzification layer	3 Gaussian Membership Functions (MFs) per input	MFO

Received: 20-10-2025 / Accepted: 13-10-2025 / Published: 13-02-2026
https://doi.org/10.70118/ujet.2026.0301.19

3	Rule firing layer	9 Rules	---
4	Normalization layer	Normalizes firing strengths	---
5	Defuzzification layer	9 Linear Output Functions	ANFIS
6	Output Summantion layer	Weighted sum (Reference current)	-

The mermaid diagram is shown in figure 11. Figure 11 shows the flow of process between the several layers in the model. It presents a graphical description of the network architecture.

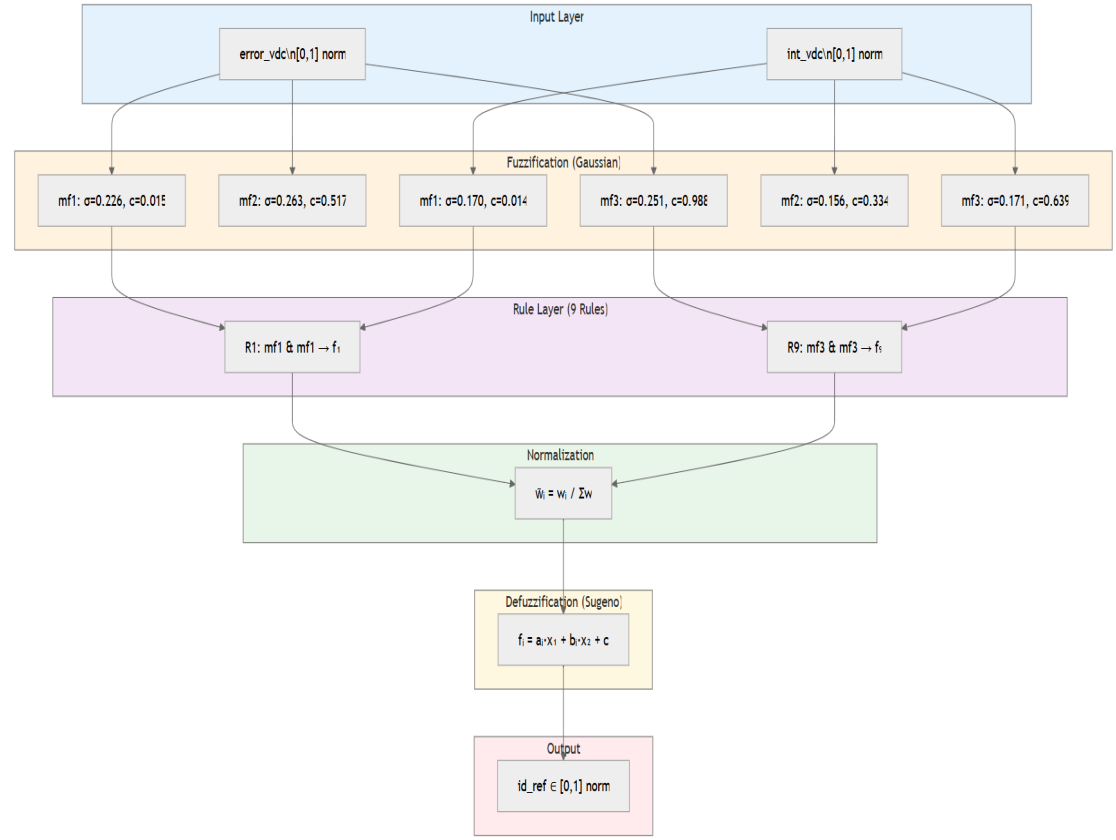

Figure 11. MFO-ANFIS architecture.

The algorithm pseudocode is :

MFO-ANFIS Algorithm Pseudocode

```
BEGIN
BEGIN MFO_ANFIS_UPQC_Control

  // PHASE 1: DATA PREPARATION
  data ← LOAD('UPQC_dataset.mat')            // [error_vdc, int_vdc, id_ref]
  data ← REMOVE_ROWS_WITH(NaN OR Inf)
     min_vals ← MIN(data, axis=0)
  max_vals ← MAX(data, axis=0)
  range_vals ← max_vals - min_vals + ε
  data_norm ← (data - min_vals) / range_vals
  SAVE(min_vals, range_vals)                 // For real-time deployment
  (trainData, valData) ← SPLIT(data_norm, ratio=0.8)
  X_val ← valData[:, 1:2], Y_val ← valData[:, 3]
  // PHASE 2: BASELINE ANFIS (Direct Training)
  baseFIS ← GENFIS(
     inputs:  trainData[:, 1:2]
     output:  trainData[:, 3]
     method:  GridPartition
```

Received: 20-10-2025 / Accepted: 13-10-2025 / Published: 13-02-2026
https://doi.org/10.70118/ujet.2026.0301.19

```
    numMFs:  3 per input
    mfType:  Gaussian
)
baseFIS ← ANFIS_TRAIN(
    FIS:     baseFIS
    data:    trainData
    epochs:  10
    validate: valData
)
baseRMSE ← EVALUATE_RMSE(baseFIS, X_val, Y_val)
SAVE(baseFIS, 'UPQC_ANFIS_DIRECT.fis')
// PHASE 3: MFO FINE-TUNING (σ Optimization)
centers ← LINSPACE(0.2, 0.8, 3)              // Fixed: [0.2, 0.5, 0.8]
nPremiseVars ← 6                             // Only σ1..σ6
lb ← [0.05, ..., 0.05] (6×)
ub ← [2.00, ..., 2.00] (6×)
nMoths ← 40, maxIter ← 60
// Initialize population near baseFIS σ
FOR each input i ∈ {1,2}
    FOR each mf j ∈ {1,2,3}
        idx ← (i-1)*3 + j
        σ_base ← baseFIS.Inputs(i).MF(j).σ
        pop[:, idx] ← σ_base + N(0, 0.1)      // Gaussian perturbation
    END
END
pop ← CLAMP(pop, lb, ub)

BestFIS ← baseFIS
BestRMSE ← baseRMSE
BestPos ← pop[1, :]

FOR iter = 1 TO maxIter
    fitness ← [∞, ..., ∞] (nMoths×)
    valid_count ← 0
    FOR moth = 1 TO nMoths
        σ_vec ← pop[moth, :]
        TRY
            fis ← BUILD_FIS(σ_vec, centers, baseFIS)
            IF NOT VALID(fis) → CONTINUE
            // 5-epoch hybrid tuning
            fis_trained ← ANFIS_TRAIN(
                FIS:    fis
                data:   trainData
                epochs: 5
            )
            Y_pred ← EVALFIS(fis_trained, X_val)
            IF ANY(NaN OR Inf IN Y_pred) → CONTINUE
            rmse ← RMSE(Y_val, Y_pred)
            fitness[moth] ← rmse
            valid_count ← valid_count + 1
            IF rmse < BestRMSE
                BestRMSE ← rmse
                BestPos  ← σ_vec
                BestFIS  ← fis_trained
            END
        CATCH
            CONTINUE
        END
    END
```

Received: 20-10-2025 / Accepted: 13-10-2025 / Published: 13-02-2026

https://doi.org/10.70118/ujet.2026.0301.19

```
    // MFO Update Mechanism
    flameNo ← MAX(1, ROUND(nMoths × (1 - iter/maxIter)))
    validIdx ← isfinite(fitness)
    IF ANY(validIdx)
      sortedIdx ← SORT(fitness[validIdx])
      flames ← pop[validMoths(sortedIdx), :]
      flames ← flames[1:flameNo, :]
    ELSE
      flames ← pop[RANDPERM(nMoths, flameNo), :]
    END
    FOR i = 1 TO nMoths
      FOR j = 1 TO nPremiseVars
        flame ← flames[MIN(i, flameNo), j]
        d ← |flame - pop[i,j]|
        t ← (a-1)×RAND + 1
        pop[i,j] ← d × exp(t) × cos(2πt) + flame
        pop[i,j] ← CLAMP(pop[i,j], lb[j], ub[j])
      END
    END
    PRINT("Iter", iter, "| Valid:", valid_count, "/", nMoths,
        "| Best RMSE:", BestRMSE)
  END
  // PHASE 4: FINAL MODEL
  SAVE(BestFIS, 'UPQC_MFO_TUNED.fis')
  PRINT("FINAL RMSE =", BestRMSE)
  // PHASE 5: DEPLOYMENT
  FUNCTION id_ref = DEPLOY(error_vdc, int_vdc)
    x_norm ← ( [error_vdc, int_vdc] - min_vals[1:2] ) / range_vals[1:2]
    y_norm ← EVALFIS(BestFIS, x_norm)
    id_ref ← y_norm * range_vals[3] + min_vals[3]
    RETURN id_ref
  END
END MFO_ANFIS_UPQC_Control
```

3.0 Results and Discussion

The description of each bus in the 33kV distribution line diagram is in Table 2.

Table 2. Buses Description for Distribution System

Bus(es)	Description
B1	Source
B2	Bus One
B3	Micro-grid
B4	After Fault
B5	Load/Pcc
B6	Injection Voltage
B7	Current from Shunt
B8	After Shunt Inductor

Figure 12. shows the source voltage and current waveform with distortion caused by the non-linear load. In this scenario, the UPQC is removed from the utility and the current values at source and Pcc (point of common coupling) measured for harmonic distortion.

Received: 20-10-2025 / Accepted: 13-10-2025 / Published: 13-02-2026
https://doi.org/10.70118/ujet.2026.0301.19

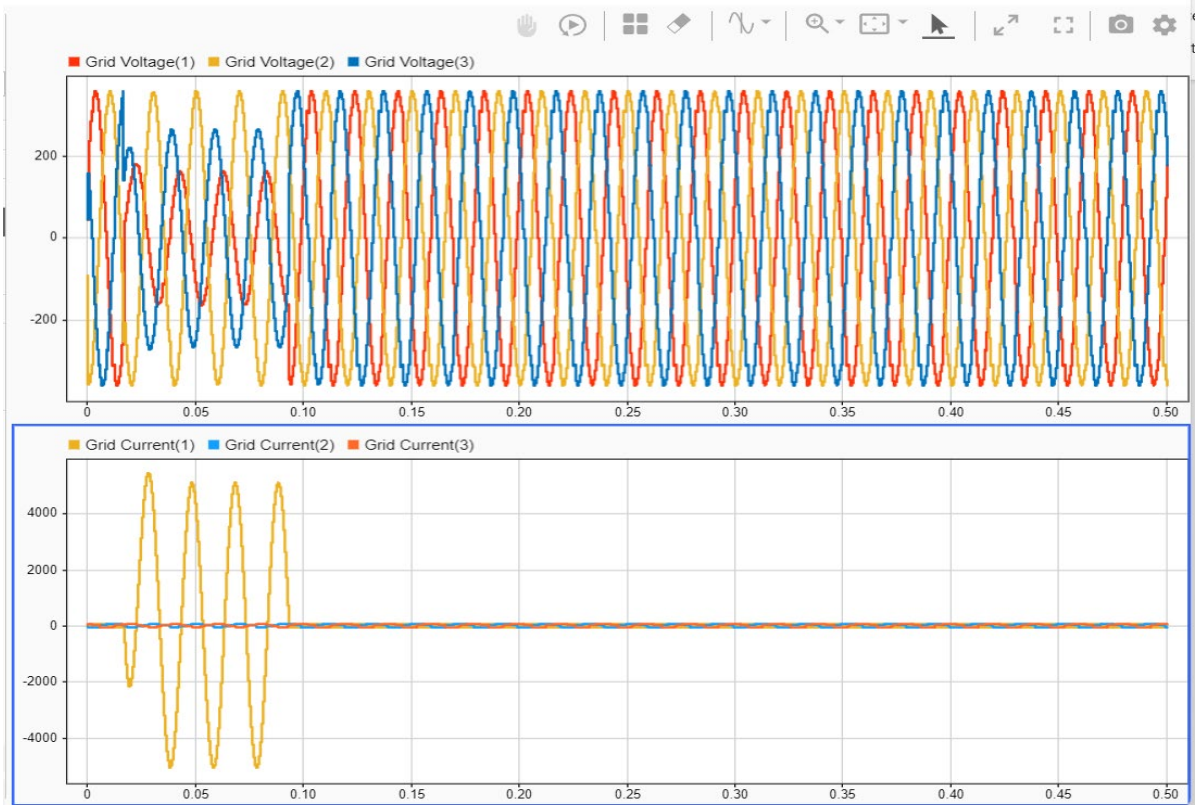

Figure 12. Grid Voltage and Current

The FFT analyzer has been used to analyse the total harmonic distortion present in the current waveforms. Figure 13 shows the FFT window and the settings used to compute the THD. The distribution is simulated for 0.5 seconds with an LG (single line to ground fault) present in phase A. From figure 13, it can be seen that the THD is 17.24% which exceeds the limits set by IEEE-519. This is due to the introduction of harmonics by the simulated fault.

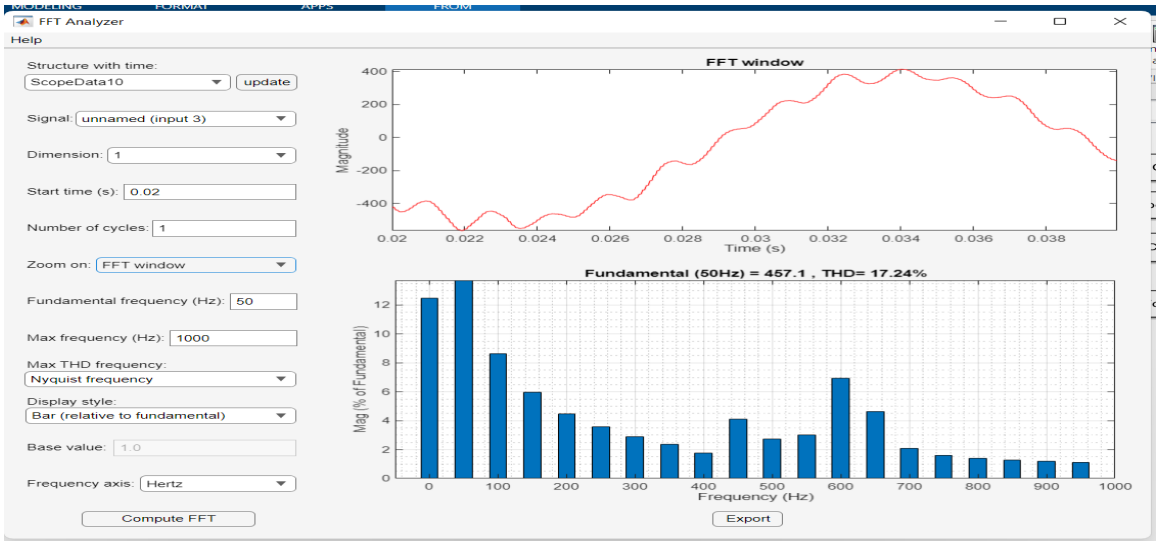

Figure 13. FFT Analyzer showing current at supply

Figures 14 was obtainable when measuring from the load side. The THD rose to 68.31% and this harmonic distortion reflects the simulated line-to-ground fault and the non-linearity of the load. This is the performance of the grid without UPQC. Any load sharing a Pcc with the non-linear load would experience harmonics and distortions.

Received: 20-10-2025 / Accepted: 13-10-2025 / Published: 13-02-2026
https://doi.org/10.70118/ujet.2026.0301.19

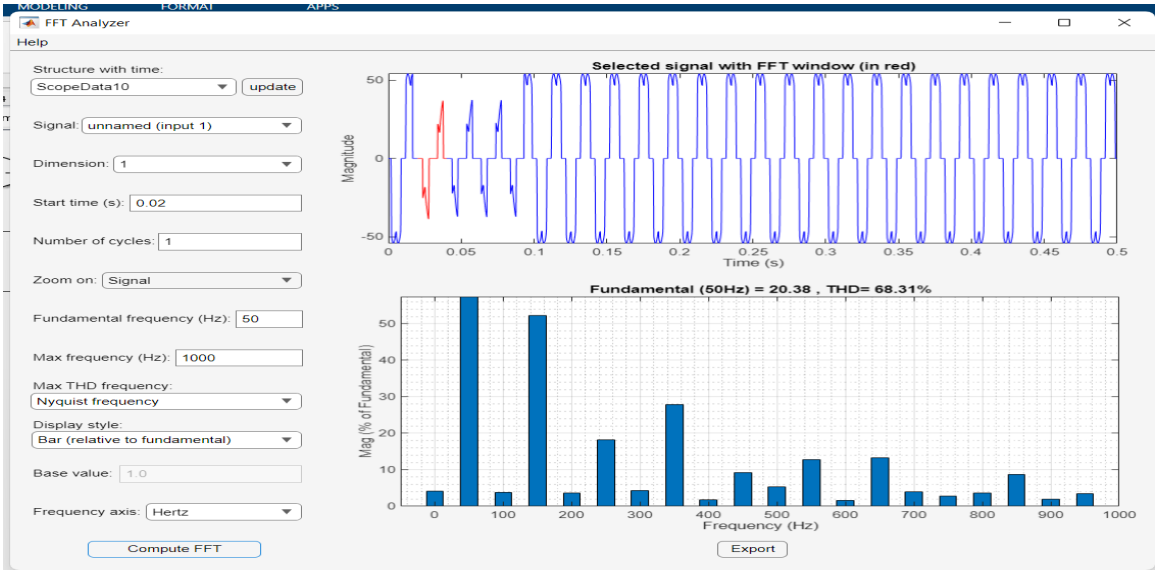

Figure 14. Pcc Current without UPQC

Figure 15 presents the Pcc current with THD. The ANFIS controller was optimized using MFO in this case. The MFO optimizes the parameters as defined by the ANFIS. The wave-forms obtained is shown in the figure below. The THD value at load Pcc using the MFO-ANFIS is 7.02%. This accounts for a 40.65% THD reduction. The harmonic distortion due to the simulated fault and non-linear load has been reduced by the UPQC with its control optimized using the MFO-ANFIS.

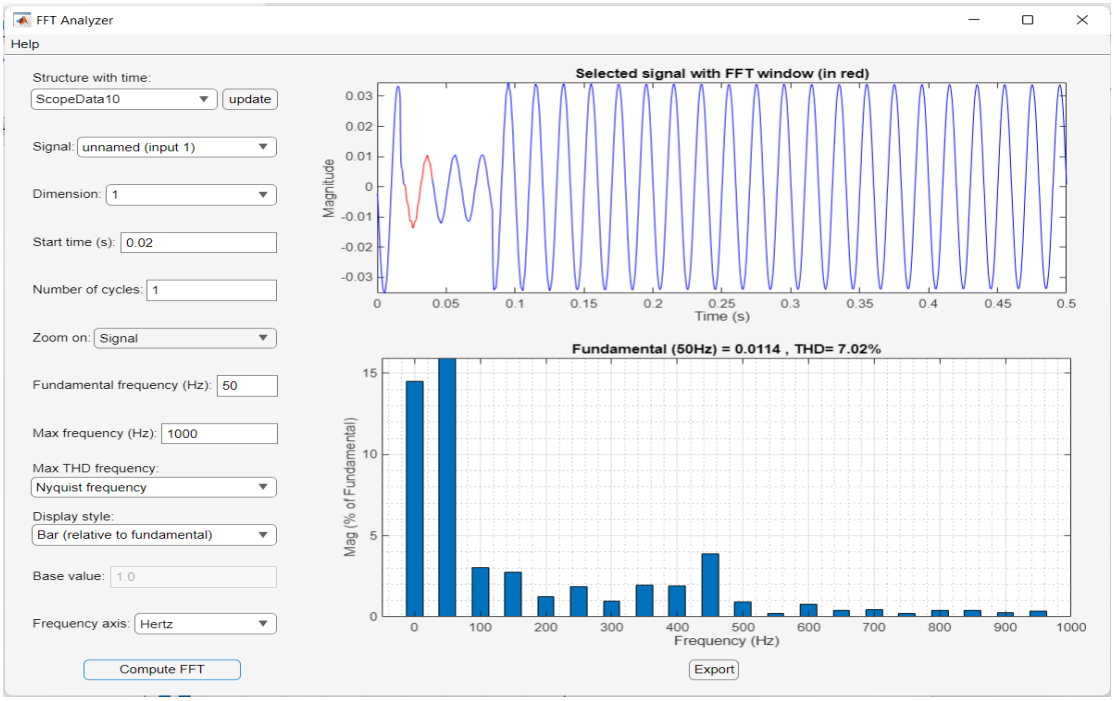

Figure 15. FFT Analyzer showing Pcc current with MFO-ANFIS.

Figure 16 shows voltage injection by the series APF to compensate the voltage. The injected voltage is shown at the point of voltage between $0 < t < 0.10$seconds. The waveform for the injected voltage drops to zero along the waveform where there are no voltage sags.

Received: 20-10-2025 / Accepted: 13-10-2025 / Published: 13-02-2026
https://doi.org/10.70118/ujet.2026.0301.19

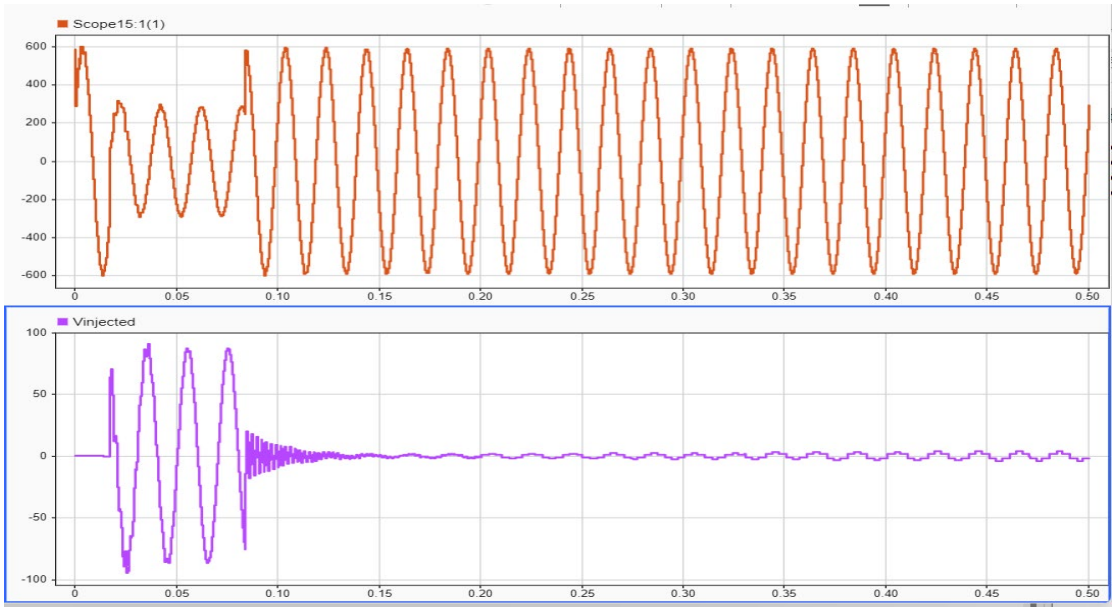

Figure 16. Source voltage (top) vs injected voltage below (below) in FFT Analyzer

The UPQC is deployed in MFO-ANFIS and no UPQC scenario. The performance of the UPQC controllers in improving line current harmonics are compared in Table 3. The comparison is in terms of total harmonic distortion (THD). According to IEEE-519 standards, the maximum THD allowable for medium voltage systems (1kV<V<69kV), is 8% for voltage and current.

Table 3. Performance Evaluation

UPQC	THD (%)	
	Current at Source	Current at Pcc
Without UPQC	17.24	68.31
MFO-ANFIS	11.83	7.02

There is an improvement in performance of a system with UPQC over one without UPQC as indicated in the massive reductions in THD by compensation from the UPQC. With MFO-ANFIS, the THD is reduced from 68.31% by 89.72%.

4.0 Conclusion

Through a comparison of three scenarios involving the UPQC, the MFO-ANFIS has shown the best performance. The THD value for the MFO-ANFIS is 7.02% which is within the IEEE-519 standards in a fault scenario. The MFO-ANFIS approach showed capability of injecting voltage into the grid for compensation.

Acknowledgements

My sincere gratitude to members of staff, Department of Electrical and Electronic Engineering, University of Abuja, and my supervisory committee under whose supervision, this study was carried out.

Availability Of Data

The data-set used for the model training is saved in a different document and would be made available upon request.

References

Afonso, J. L., Tanta, M., Pinto, J. G. O., Monteiro, L. F. C., Machado, L., Sousa, T. J. C., & Monteiro, V. (2021). A review on power electronics technologies for power quality improvement. *Energies*, *14*(8585), 1 - 71. https://doi.org/10.3390/en14248585.

Alrashad, M. M., Flah, A., Dashtdar, M., El-Bayeh, C. Z., & Elnaggar, M. F. (2024). Improving the control strategy of the DVR compensator based on an Adaptive Notch filter with an optimized PD controller using the IGWO algorithm. *Int. Trans. on Elect. Ener. Syst., Wiley, 2024,* 1 - 32. https://doi.org/10.1155/2024/5097056.

Amini, M., & Alireza, J. (2020). Optimal sizing and location of open-UPQC in distribution networks considering load growth. *International Journal of Electrical Power and Energy Systems*, 106893. https://doi.org/10.1016/j.ijepes.2021.106893.

Received: 20-10-2025 / Accepted: 13-10-2025 / Published: 13-02-2026

https://doi.org/10.70118/ujet.2026.0301.19

Benachaiba, C., Abdelkhalek, O., Dib, S., Allali, M., & Dib, D. (2014). The unified power quality conditioner (UPQC): The principle, control and application. In *Proceedings of the Power Conversion Conference* (pp. 1–5). https://doi.org/10.1109/PCC.2002.998518.

Bharathi, S. A., Sudhakara, R., & Damodar, R. M. (2017). Optimal placement of UPFC and SVC using moth-flame optimization algorithm. *International Journal of Electrical and Computer Engineering, 7*(5), 2472–2479.

Biricik, S. (2018). Design of unified power quality conditioner for power quality improvement in distribution network. *International Journal of Research Studies in Electrical and Electronics Engineering, 4*(2), 1–9.

Cek, J. (2018). Protection and power quality in distributed generation interfaced fuel cell. *Journal of Electrical Power Systems Research, 13*(2).

Chaiyaphun, K., Santiprapan, P., & Areerak, K. (2024). A modified variable power angle control for unified power quality conditioner in a distorted utility source. *Energies*, *17*(2830), 1 - 18. https://doi.org/10.3390/en17122830.

Dash, S. K., & Pravat, K. R. (2021). Power quality improvement utilizing PV fed unified power quality conditioner based on UV-PI and PR-R controller. *CPSST Transactions on Power Electronics and Applications.* https://doi.org/10.24295/CPSSTPEA.2018.00024.

Dharmalingam, R., Subhransu, S. D., Karthikrajan, S., Arun, B. M., & Subramani, C. (2014). Power quality improvement by unified power quality conditioner based on CSC topology using synchronous reference frame theory. *Hindawi Publishing Corporation Journal of Power Electronics, 2014.*

Hosseini, S., & Mehdi. (2018). The operation and model of UPQC in voltage sag mitigation using EMTP by direct method. *Journal of Electrical Systems, 2*(3), 148–156.

Huang, Z., Shahbaazy, F., & Davarpanah, A. (2022). A unified power quality conditioner for feeder reconfiguration and setting to minimize the power loss and improve voltage profile. *Hindawi Journal*, 2022, 1–8. https://doi.org/10.1155/2022/5742846.

Kenjrawy, H., Makdisie, C., Houssamo, I., & Mohammed, N. (2022). New modulation technique in smart grid interfaced multi-level UPQC-PV controlled via fuzzy logic controller. *Electronics, 11*(9), 919. https://doi.org/10.3390/electronics11060919.

Mahdi, D. I., & Gorel, G. (2022). Design and control of three-phase power system with wind power using unified power quality conditioner. *Energies, 15*(19), 7074. https://doi.org/10.3390/en15197074.

Mirjalili, S. (2015). Moth-flame optimization algorithm: A novel nature-inspired heuristic paradigm. *Knowledge-Based Systems.* https://doi.org/10.1016/j.knosys.2015.07.006

Mishra, R. S., & Kumar, P. (2017). Survey on voltage improvement. *IJSRD*, *5*(2017), 557 - 560.

Mohamed, A. O., Almelian, M. M., Izzeldin, I. M., & Usman, U. S. (2018). Performance of unified power quality conditioner (UPQC) based on fuzzy controller for attenuating voltage and current harmonics. *Journal of Electrical Engineering, 342.*

Nicola, M., Nicola, C.-I., Sacerdotianu, D., & Vintila, A. (2023). Comparative performance of UPQC control scheme based on PI-GWO, fractional order controllers, and reinforcement learning agent. *Electronics, 12*(494), 1–22. https://doi.org/10.3390/electronics12030494.

Srimatha, S., Mallala, B., & Upendar, J. (2023). A novel ANFIS-controlled customized UPQC device for power quality enhancement. *Journal of Electrical Systems and Information Technology, 10*(55). https://doi.org/10.1186/s43067-023-00121-1.

Sundarabalan, C. K., Puttagunta, Y., & Vignesh, V. (2019). Fuel cell integrated unified power quality conditioner for voltage and current reparation in four-wire distribution grid. *IET Smart Grid*, *2*(1), 60 - 68. https://doi.org/10.1049/iet-stg.2018.0418.

Tarani, K. S., Sita, K., & Anala, A. (2018). Improvement of power quality using unified power quality conditioner for a grid-connected PV system. *International Journal of Research and Reviews, 5*(3), 617–622.

Xia, M., & Li, X. (2013). Design and implementation of a high quality power supply scheme for a distributed generation in a micro-grid. *Energies, 6*(9), 4924–4944. https://doi.org/10.3390/en6094294.

Received: 20-10-2025 / Accepted: 13-10-2025 / Published: 13-02-2026

https://doi.org/10.70118/ujet.2026.0301.19